NANO MICRO small

Rapid, High-Throughput, and Direct Molecular Beacon Delivery to Human Cancer Cells Using a Nanowire-Incorporated and Pneumatic Pressure-Driven Microdevice

Kyung Hoon Kim, Jung Kim, Jong Seob Choi, Sunwoong Bae, Donguk Kwon, Inkyu Park, Do Hyun Kim, and Tae Seok Seo**

***T**racking and monitoring the intracellular behavior of mRNA is of paramount importance for understanding real-time gene expression in cell biology. To detect specific mRNA sequences, molecular beacons (MBs) have been widely employed as sensing probes. Although numerous strategies for MB delivery into the target cells have been reported, many issues such as the cytotoxicity of the carriers, dependence on the random probability of MB transfer, and critical cellular damage still need to be overcome. Herein, we have developed a nanowire-incorporated and pneumatic pressure-driven microdevice for rapid, high-throughput, and direct MB delivery to human breast cancer MCF-7 cells to monitor survivin mRNA expression. The proposed microdevice is composed of three layers: a pump-associated glass manifold layer, a monolithic polydimethylsiloxane (PDMS) membrane, and a ZnO nanowire-patterned microchannel layer. The MB is immobilized on the ZnO nanowires by disulfide bonding, and the glass manifold and PDMS membrane serve as a microvalve, so that the cellular attachment and detachment on the MB-coated nanowire array can be manipulated. The combination of the nanowire-mediated MB delivery and the microvalve function enable the transfer of MB into the cells in a controllable way with high cell viability and to detect survivin mRNA expression quantitatively after docetaxel treatment.*

K. H. Kim, J. S. Choi, S. Bae, Prof. D. H. Kim, Prof. T. S. Seo
Department of Chemical and Biomolecular Engineering
Korea Advanced Institute of Science and Technology
Daejeon 305–701, Korea
E-mail: seots@kaist.ac.kr

J. Kim, D. Kwon, Prof. I. Park
Department of Mechanical Engineering
Korea Advanced Institute of Science and Technology
Daejeon 305–701, Korea
E-mail: inkyu@kaist.ac.kr

DOI: 10.1002/smll.201502151

1. Introduction

Over the last decades, great advances have been made in biological imaging technology for better detection and characterization of abnormal cells, tissues, and disease-related cellular behaviors. In particular, monitoring specific RNA sections in living cells is essential to understand the interpretation of genetic information and its translation to proteins. In addition, abnormal gene expression of specific RNA can be an indicator of biological irregularity. Thus, the imaging, tracking, and monitoring of biomolecules such as mRNA in the intracellular environments are invaluable for evaluating chemical, spatial, and physical phenomena in cell biology, as

well as for applications in the diagnostic and medical fields. Furthermore, quantification of mRNA by fluorescence imaging can provide the information on the expression level of target mRNA or even provide insight into the progress of the disease. To observe intracellular mRNA dynamics, adequate probes need to be designed and delivered inside the cells to discriminate the target mRNA with high specificity.

Among the reported methods for sensing and analyzing mRNA, in vivo mRNA detection by molecular beacons (MBs) has been extensively explored. A molecular beacon is a stem-and-loop structured, dual-labeled, single-stranded oligonucleotide probe retaining a fluorophore and a quencher. The hairpin structure causes a quenching of the fluorophore, because of the close proximity between the fluorophore and the quencher. In the presence of target mRNA the structure is opened by hybridization of the loop sequence with the target DNA or RNA, thus restoring the fluorescence signal. The target mRNA can therefore be determined and tracked by the fluorescence signal of the MB, and the expression level of the mRNA can be quantitatively evaluated by measuring the fluorescence intensity of the MB.

Many strategies to deliver MBs into the cells have been proposed. A microinjection method was developed for direct MB delivery, but this requires special equipment for precise cell manipulation and expertise skills through prolonged training, and suffered from low throughput and low efficiency due to the time-consuming process.[1–4] An electroporation method has also been proposed in order to overcome the low delivery efficiency by using an electric stimulus,[5–9] but, this technique also has a theoretical limitation as it depends on probability-based gene delivery. Gold nanoparticles have been researched as novel delivery vehicles for MBs because of their inertness and low cytotoxicity. In comparison to the other methods, the use of gold nanoparticles successfully protected the MBs from nuclease degradation.[10] Seferos et al.[11] reported a nanoflare-type of gold nanomaterial, on which single and short oligonucleotides were conjugated to recognize target mRNA sequences. Yeh et al.[12] linked a MB on the surface of the quantum dots and gold nanoparticles, which were utilized as intracellular delivering cargos. Lin et al.[13] demonstrated the delivery of a polymer-conjugated MB into mammalian cells with minimized degradation of the MB in the cells. However, these nanomaterial-based and carrier-oriented delivery systems rely on endocytosis-dependent internalization, which requires long incubation times for the vehicle penetration into the cells. Moreover, these nanocarrier-based delivery techniques can cause cross-contamination and have correlated intracellular cytotoxicity issues.

On the other hand, nanowires have also displayed unique characteristics, for instance, strong mechanical properties, facile functionalization, and size controllability, which are useful for gene delivery.[14,15] The nanowire-mediated delivery of gene-encapsulated nanoparticles into a mouse model and the quantification of nanowire penetration into living cells have been studied.[16] The interactions between cells and nanowires has been explored, as well silicon nanowires-based gene delivery to mammalian cells.[17] Nanowire-based delivery, however, has hitherto shown limitations in terms of the prolonged cellular penetration step, as the cell adhesion on the nanowire array solely depends on gravity. Moreover, the cell recovery from the nanowire array was executed by chemical treatment, such as with trypsin- ethylenediaminetetraacetate (EDTA), which deteriorates the cellular viability for downstream cell research. The lack of controllability over the cellular manipulation, such as attachment and detachment from the nanowires, also remains a challenge to be overcome, which is of importance for achieving precise gene delivery by the nanowire method.

In this study, we present a nanowire-incorporated microdevice for controlled MB delivery to cells. In addition to the incorporation of ZnO nanowires, the microdevice was equipped with a pneumatic microvalve, which could manipulate the cellular interaction with the nanowire array. Thus, the combination of the nanowire and the pneumatic microvalve enabled us to perform rapid and high-throughput MB delivery, as well as cell recovery. As a model, we employed a MB probe that targeted survivin mRNA and evaluated the expression level of the survivin mRNA in human breast-cancer MCF-7 cells.[18] The MBs that were delivered to the cells by the pneumatic microvalve function could successfully quantify survivin mRNA in the cells depending on the docetaxel dose.

2. Result and Discussion

2.1. Fabrication and Operation of the Nanowire-Incorporated Microdevice

Figure 1A illustrates the schematics of the nanowire-incorporated microdevice. The top panel shows the synthetic process of the ZnO nanowires in the microchannel, and the bottom panel displays the microdevice consisting of three layers (left) and a close-up on the manifold layer (right). The microfluidic channel in the bottom layer was fabricated on a glass wafer via conventional photolithography, and the ZnO nanowires were hydrothermally grown inside the channel. The microdevice was composed of three layers: from top to bottom: a glass manifold, a monolithic polydimethylsiloxane (PDMS) membrane, and the ZnO nanowire-incorporated glass channel layer. The top glass manifold layer was prepared by wet-etching lithography, and the glass manifold and PDMS membrane functioned as a pneumatic microvalve. The manifold layer contained the solution inlet hole and outlet hole, through which the solution flowed into the microchannel in the bottom channel layer. Another pump hole, which was linked to the ellipse-shaped pneumatic chamber, was connected to an external pump system, and air or vacuum was supplied in the pneumatic chamber to deflect the PDMS membrane. The middle PDMS membrane (thickness: 250 μm) was punched and the holes were aligned with the inlet and outlet hole of the manifold to introduce the cell solution into the bottom channel layer (width: 500 μm, length: 3 cm, depth: 35 μm), in which the hydrothermally synthesized nanowires were contained.

Figure 1B describes the overall processes of the gene delivery into the cells using the proposed microdevice. First, the human breast cancer MCF-7 cells (2.5×10^5 cells mL^{-1}) were injected through the inlet hole with a syringe pump

DOI: 10.1002/smll.201502151

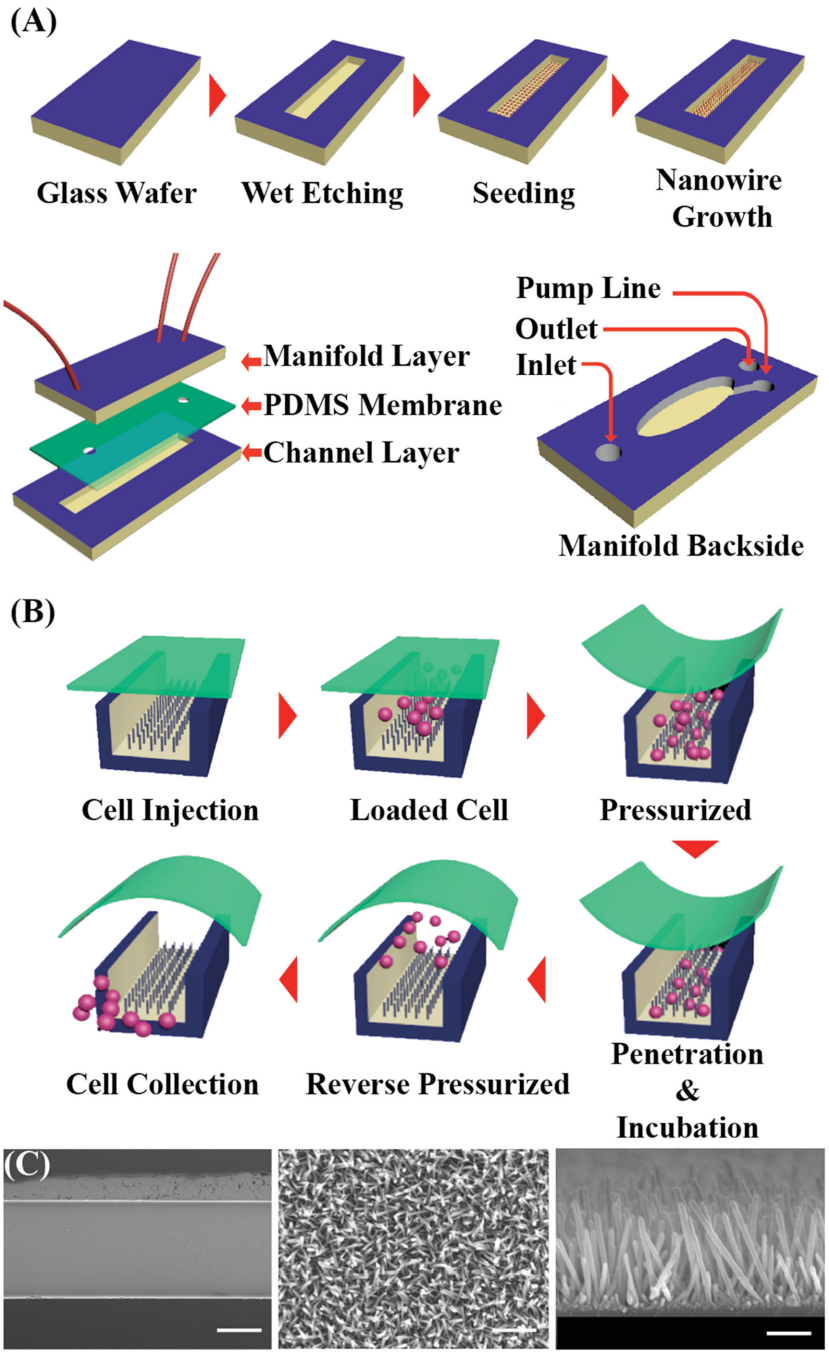

Figure 1. A) Fabrication of the nanowire-incorporated microdevice (top). The dismantled microdevice consisting of a manifold, a monolithic PDMS membrane, and a nanowire-incorporated channel layer (bottom left). Schematics of the manifold (bottom right). B) The overall process for the MB delivery from the nanowires into the cells through the pneumatic pump operation. C) SEM images of: from left to right: the top view of the nanowire-patterned microchannel, the nanowires, and a side view of the nanowires. Scale bars are 200 μm, 500 μm, and 200 μm, respectively.

and the cells were loaded in the microchannel of the bottom layer. The introduced volume was approximately 0.525 μL and approximately 131 cells were loaded into the channel. The injected cell number could be controlled by tuning the cell concentration. Once the cells were loaded, the PDMS membrane was moderately bent down by supplying air through the pneumatic pump line in the manifold. The cells were squeezed down toward the ZnO nanowires that were coated with the MB probes, and penetrated. In order to remove the floating cells that had not been pierced onto the nanowires, a cell culture media solution was injected to the channel to wash them away. The pierced cells were incubated for a while to deliver the MB on the nanowires into the cells. After MB delivery, a vacuum was applied through the pump line to make the PDMS membrane bend upwards, so the reverse-directional pressure induced a detaching of the pierced cells from the nanowires. Then, the MB-delivered cells were collected from the outlet by injecting a media solution in the inlet line for further cell cultivation.

Figure 1C shows scanning electron microscopy (SEM) images of the synthesized nanowires in the channel layer. From left to right, images for the top view of the channel, an enlarged nanowire view, and a side view of the nanowires are displayed. The hydrothermal growth of the ZnO nanowires was performed using four steps: 1) crystalline seed formation on the glass substrate, 2) seed growth by aggregation of zinc ions, 3) surface stabilization by hexamethylenetetramine (HMTA), and 4) one-dimensional growth of nanowires.[15] To produce nanowires with high aspect ratios, HMTA served as a capping agent to suppress the lateral growth of the nanowires.[19] The diameter and angle of the nanowires could be controlled by the seed preparation.[14,20] Herein, we chose a sputtering method to reduce the diameter of the nanowires, because a small diameter (average diameter: 36.8 nm) of the nanowires minimizes the cellular damage during MB delivery. Most of the nanowires were grown almost vertically with an average angle of 79.1° ± 7.0°, which was enough to penetrate the cell membrane. The length of the nanowires was tunable depending on the synthesis time. Figure 1C shows the resulting nanowires in the microchannel, whose average length was about 529.5 nm. This nanowire length was long enough to pierce the cell membrane during the pressurization process without breaking the nanowires.

2.2. Conjugation of the Molecular Beacon Probes on the Nanowires

For the MB delivery to the cells, the MB probe needs to be conjugated on the surface of the nanowires. **Figure 2**A

DOI: 10.1002/smll.201502151

www.MaterialsViews.com

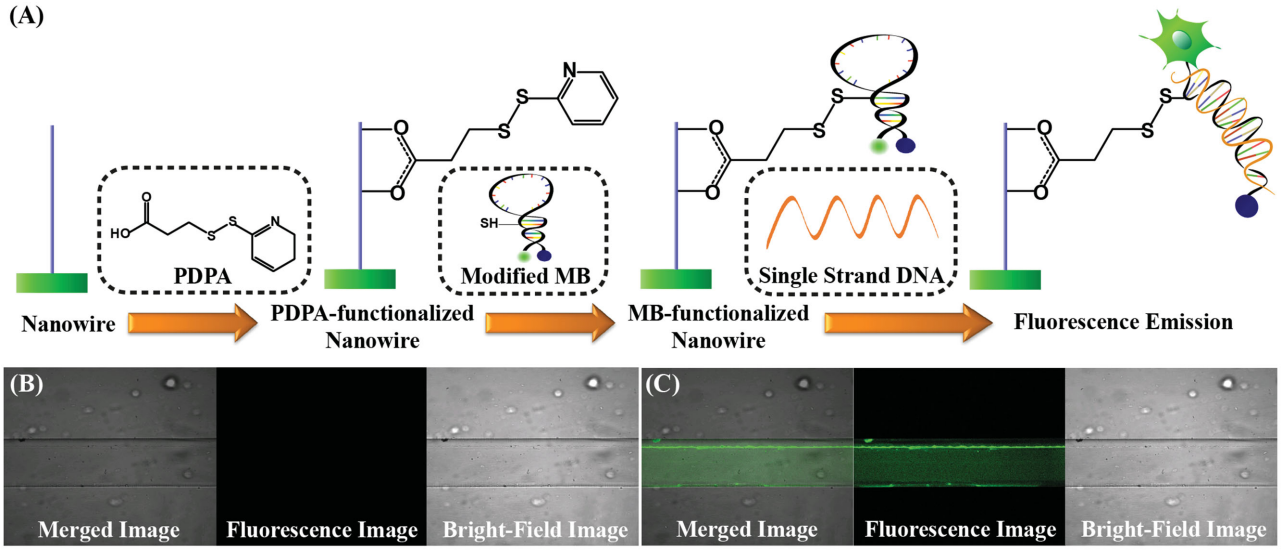

Figure 2. A) MB immobilization on the nanowires and MB hybridization with the target mRNA. B) Images of the MB modified nanowires in the microchannel. C) Microscopic images of the MB modified nanowires after hybridization with the complementary DNA. From left to right, a merged image, a fluorescence image, and a bright-field image.

describes the functionalization process to immobilize the MB on the nanowires.[21,22] The ZnO nanowires were first treated and coated with 3-(2-pyridyldithio)propanoic acid (PDPA) by covalent bonding.[22] As the PDPA contains a disulfide bond with a pyridyl leaving group, the PDPA moiety can react with a thiol functional group of MB through a disulfide exchange reaction. Thus, the MB was designed to include a thiol group in the stem part, so that the MB was immobilized on the nanowire by the disulfide bond. To confirm the fixation of the MB on the nanowires, we utilized a single-stranded complementary DNA whose sequence was matched with the loop part of the MB. Once the complementary DNA was hybridized with the MB on the wire, the fluorescence signal was revealed, which could be verified by a confocal microscope.

Figure 2B shows the MB-coated nanowires in the microchannel. As the MB initially forms a stem–loop structure in absence of target DNA, which causes a close spatial proximity of the fluorophore and the quencher, the emission of the fluorescent signal was strongly prohibited. However, when the target DNA was added to the MB-modified nanowire, target hybridization occurred, producing a green fluorescence signal in the channel due to the open structure of the molecular beacon (Figure 2C). These results imply that the MB was successfully linked on the ZnO nanowire and its functionality was retained.

2.3. Cleavage of the Molecular Beacon Probes from Nanowires

Scheme 1 shows the MB delivery mechanism from the nanowires to the human breast cancer MCF-7 cells. When the cells are penetrated by the MB-functionalized nanowires with the assistance of a pneumatic pump system, the MB on the nanowires are positioned inside of the cells. Due to the highly reducing environment of the cytosol, the disulfide chemical bonds between the molecular beacons and the nanowires are cleaved during incubation.[23] Then, the released MB encounters the target survivin mRNA in the cytosol. Although the cell membrane is slightly damaged due to the nanowire penetration the nanowire-induced pore is relatively small compared to the whole cell size. As the force that holds the stem–loop structure of MB is weaker than that of the double-stranded helix formed between the MB and the target mRNA, the MB turns into its linear form, which results in the spatial separation between the fluorophore and the quencher, causing the emission of the green fluorescent signal.

2.4. Cell Viability with Pressure Variation

During the penetration of the nanowires into the cells, it is essential to control the pressure to minimize the cell damage. **Figure 3**A,B shows the cellular morphological change with varying pressure. Five different pressure conditions (0 mbar, 4.4 mbar, 13 mbar, 40 mbar, 124 mbar) were applied to the manifold, and the bending degree of the PDMS membrane was amplified in proportion to the exerted pressure. To be able to visualize the cellular morphology, the cell membrane was stained with a red color using 1,1′-dioctadecyl-3,3,3′,3′-tetramethylindocarbocyanine perchlorate (Dil).[24] Under each pressure condition, we examined the cell membrane status and carried out a cell viability assay. No significant morphological changes were observed between 0 mbar (control) and 4.4 mbar pressure. In reality, a pressure of 4.4 mbar was too weak to hold the cells in place, so the majority of the cells was removed during the washing step. The cell viability at 4.4 mbar was 92.3% on average. At a pressure of 13 mbar, the cellular size was noticeably enlarged, and throughout the process the cells were penetrated by the nanowires. The cell viability at 13 mbar was 83% on average. On the other hand,

DOI: 10.1002/smll.201502151

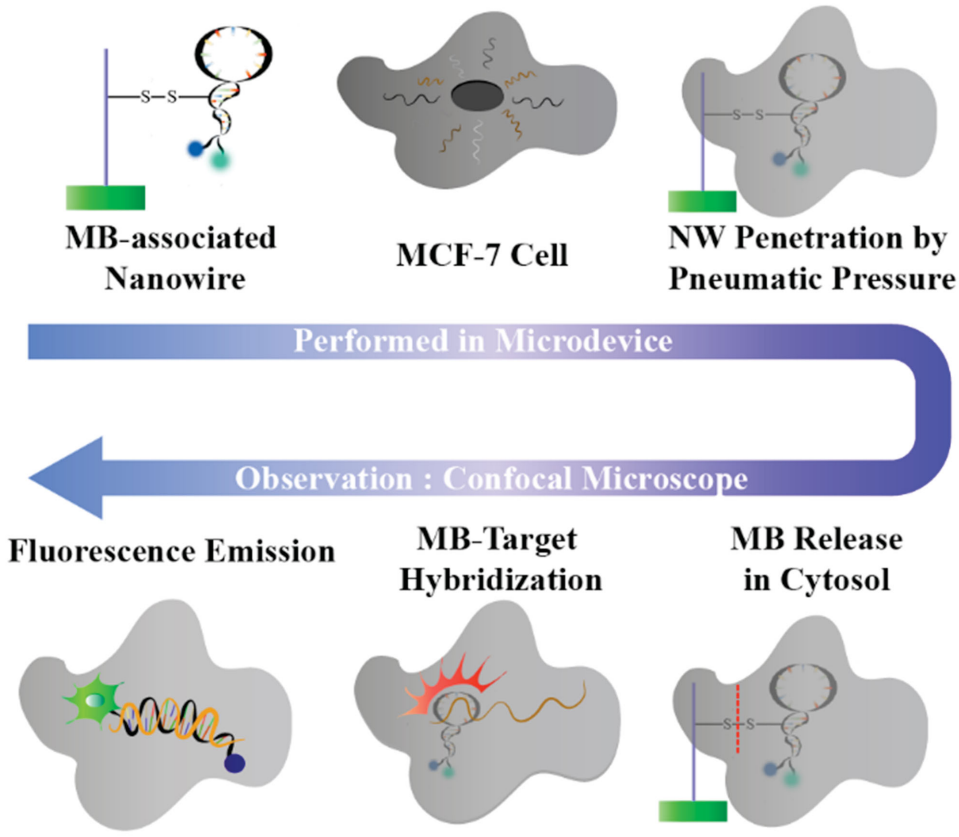

Scheme 1. Schematics of the molecular beacon delivery from the nanowires into the cells and the molecular beacon hybridization with the target gene in the cytosol.

pressures of 40 mbar and 124 mbar enforced the cells to be held tightly with significant morphological changes. However, these conditions were detrimental to the cells, revealing a lower viability and higher mortality as shown in Figure 3C. These experimental results uphold the necessity for determining optimal pressure conditions to avoid cell membrane rupture. Considering the cellular fixation and the viability, we decided that 13 mbar was suitable for the MB delivery step.

However, the delivered number of MBs still needed to be checked. We therefore performed tests to determine the MB-delivery efficiency depending on the degree of pneumatic pressure with the same MB-functionalized nanowire array to evaluate the relationship between the applied pressure and the delivery efficiency of MB into the cells. Because 0 mbar and 4.4 mbar were too weak to hold the cells, we only used the controlled pressure variations of 13 mbar, 40 mbar, and 124 mbar. As the applied pressure was increased, the fluorescent intensity of the cells augmented, implying that the delivery efficiency of the MB is proportional to the applied pressure (Figure 3D and 3E). The MB delivery efficiency at 40 mbar and 124 mbar was higher than that at 13 mbar by about 5.89-fold and 9.19-fold, respectively. However, as shown in Figure 3C, the cell viability percentage was significantly reduced at 40 and 124 mbar, so 13 mbar was deemed adequate as a certain number of MBs was still transferred to the cytosol to monitor the mRNA.

2.5. Comparison of Cell Cultivation

After the MB was delivered to the cells at 13 mbar pressure, the cells were collected and cultured. **Figure 4** shows the proliferation rate of cells that underwent MB delivery under 13 mbar and 0 mbar (a control sample). The time-lapse cell-culture images show that the cell proliferation rate at which the MB was delivered to the cells at 13 mbar was slower than that of the control probably due to the nanowire-induced damages. However, the cell culture was maintained and the coverage area was 70–80% of that of the control sample after 2 days. As the cultivation time was prolonged, the MB-delivered cells kept growing to 70% yield of the control. These results suggest that the MB can be injected into the human breast cancer MCF-7 cells at moderate pressure, and the nanowire-induced physical damage is not significant for cell viability.

2.6. Imaging and Quantification of Survivin mRNA Expression Level

Although the time for disulfide bond cleavage inside cells has been previously reported,[21] the toxicity and mechanical damage induced by the ZnO nanowires cannot be neglected in this process. Thus, we measured the fluorescence intensity of the pressurized cells over time to find the optimal injection

DOI: 10.1002/smll.201502151

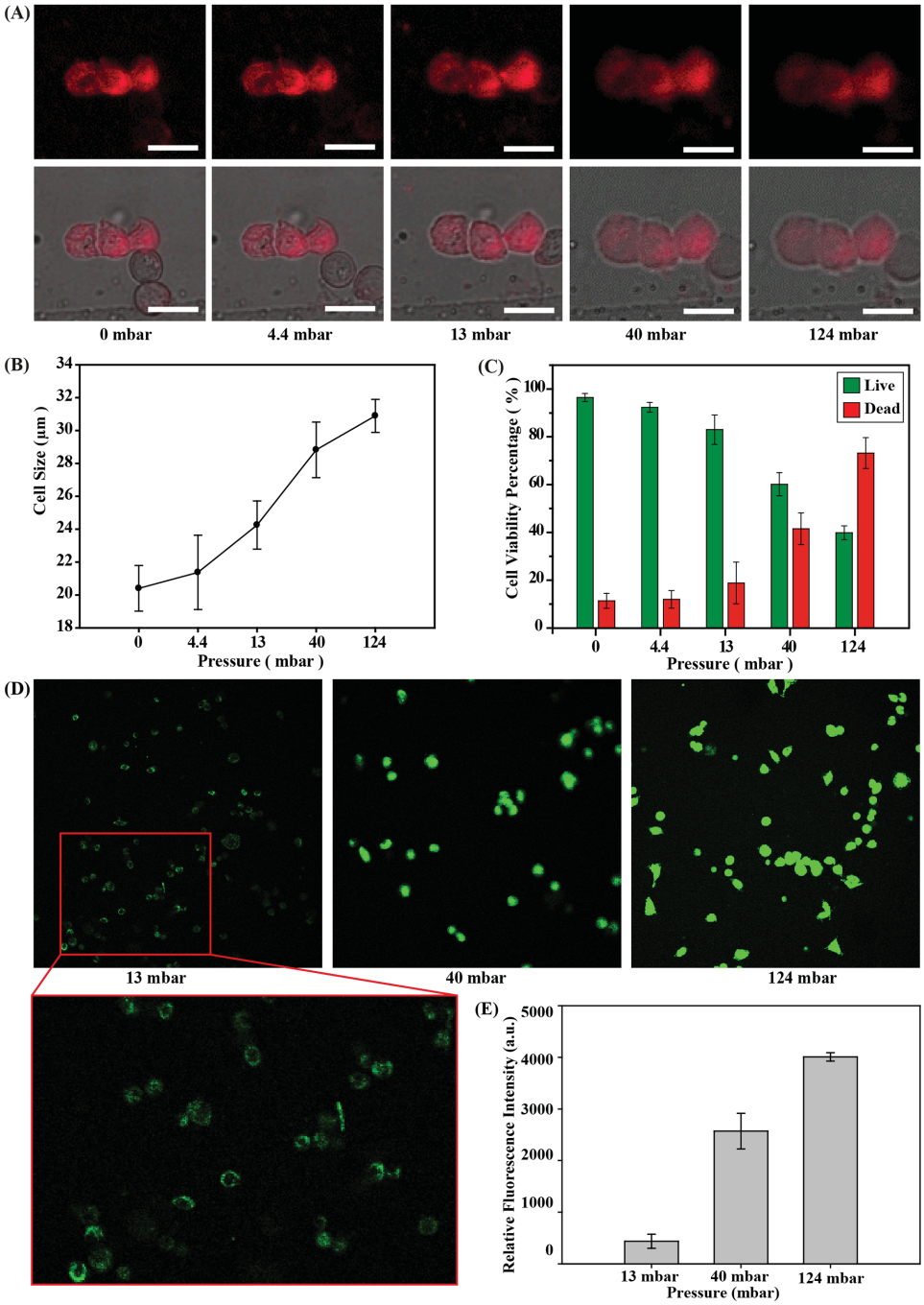

Figure 3. A) Morphological change of Dil-stained MCF-7 cells under 5 different pressures (0 mbar, 4.4 mbar, 13 mbar, 40 mbar, 124 mbar). Scale bar: 20 μm. B) Plot of the variation in cell size depending on the applied pressure. C) Cell viability percentage in relation to the applied pressure. D) Fluorescence images of the MB-delivered cells depending on the applied pressure. E) Quantitative analysis of the relative fluorescence intensity of the cells versus the applied pressure.

time. **Figure 5**A shows that the fluorescence signal remained low for the first 20 min. After 20 min, the fluorescence intensity of the cells slightly increased, and between 30 and 35 min the fluorescence signal had notably augmented. Finally the signal was saturated after 40 min. Therefore, we selected 35 min as an incubation time to cleave the MB quantitatively and to reduce the possible toxicity and membrane damage by the nanowires.

To evaluate whether the delivered MB can perform the quantitative analysis of the target survivin mRNA, we treated the MCF-7 cells with docetaxel, which leads to up-regulation of the survivin gene expression.[25,26] Cells were incubated in Dulbecco's modified eagle's medium (DMEM) containing docetaxel for 10 h, and the concentration of docetaxel was controlled at 0 nM, 1 nM, 10 nM, and 50 nM. Then, MB delivery was carried out via the same procedure as before

DOI: 10.1002/smll.201502151

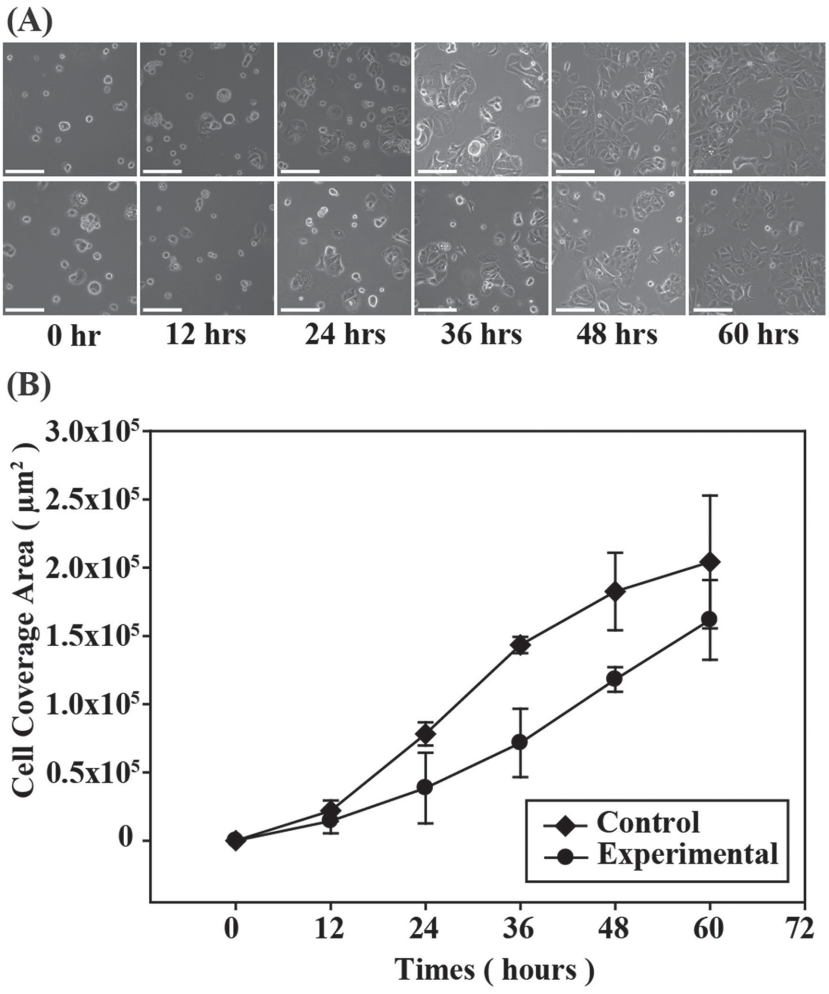

Figure 4. A) Time-lapse images of the cultured cells. The top panels are images of a control sample and the bottom panels are images of the experimental sample (13 mbar). Scale bar: 50 μm. B) Comparison of cell coverage areas of a control sample and an experimental sample (13 mbar) up to a cultivation time of 60 h.

using the nanowire-incorporated microdevice. The MB-delivered cells were recovered and their fluorescence was measured by calculating the average intensity per unit area (μm^2). The fluorescence intensity level was gradually enhanced in proportion to the increased concentration of docetaxel due to the augmented survivin gene expression (Figure 5B). These results confirm that the relative amount of survivin mRNA could be quantified by the delivered MBs. Figure 5C displays green fluorescence images of MB-delivered cells according to the docetaxel concentration. As the concentration increased, the fluorescence intensity of the cells also became higher.

To examine the selectivity for detecting survivin mRNA, we also performed an identical experiment with a normal cell and one with a smooth muscle cell (SMC) as a model. Due to the high expression level of survivin mRNA in the tumor cells, the MCF-7 cells showed a much higher fluorescence intensity than the SMC by about 3.09-fold (Figure S1, Supporting Information). These results imply that we could monitor any target mRNA in the cells by designing the MB sequence such that it is specific to the target mRNA.

2.7. Verification of the Nanowire-based MB Delivery

According to a report of Perrier-Cornet, the cell-membrane permeability can be enhanced by the applied pressure on the cells.[27] Thus, we hypothesized that floating MBs, which might be released from the nanowires, could be undesirably delivered to the cells by the pressurization. To prove this hypothesis of pressure-induced delivery, we compared the fluorescent intensity of the cells after MB delivery on the nanowire-fabricated microchannel with that of the microchannel without nanowires (as a negative control). The MB was immobilized on the ZnO nanowires or on the glass surface through the PDPA linker, and the unconjugated MBs were washed away. Under identical conditions, the same number of cells was loaded and MB delivery was actuated by applying 13 mbar. The cells were recovered and their fluorescence intensity was measured as shown in **Figure 6**. The nanowire-mediated MB-delivered cells revealed a 3-fold higher fluorescence intensity than the cells into which the MBs were delivered solely by pressure. These results imply that the intracellular MB delivery by the nanowire-incorporated and pneumatic pressure-driven microdevice was accomplished mainly by the nanowire punctuation into the cells. Furthermore, we evaluated the relative delivery efficiency of MB into the cells by comparing the fluorescence intensity in the nanowire channel before and after MB delivery to the cells. After the cell attachment on the MB-coated nanowires under 13 mbar for 35 min, the cells were removed by applying the reverse-directional pressure. Then, we added complementary single-stranded DNA to induce hybridization with the remaining MBs in the channel, so that we could compare the fluorescence intensity of the channel background with that of the cell attached position. As described in Figure S2 (Supporting Information), the cell attached position could be recognized by the circular black dots. The fluorescence intensity of the black dots was 38.58 a.u., whereas that of the channel background was 94.33 a.u., revealing that the MB-delivery efficiency was 59.1% on average.

3. Conclusion

We developed a rapid and direct MB-delivery microdevice. The combination of the ZnO nanowire arrays with the pneumatic pump system enabled high-throughput MB delivery as well as cellular manipulation. The degree of the cellular

DOI: 10.1002/smll.201502151

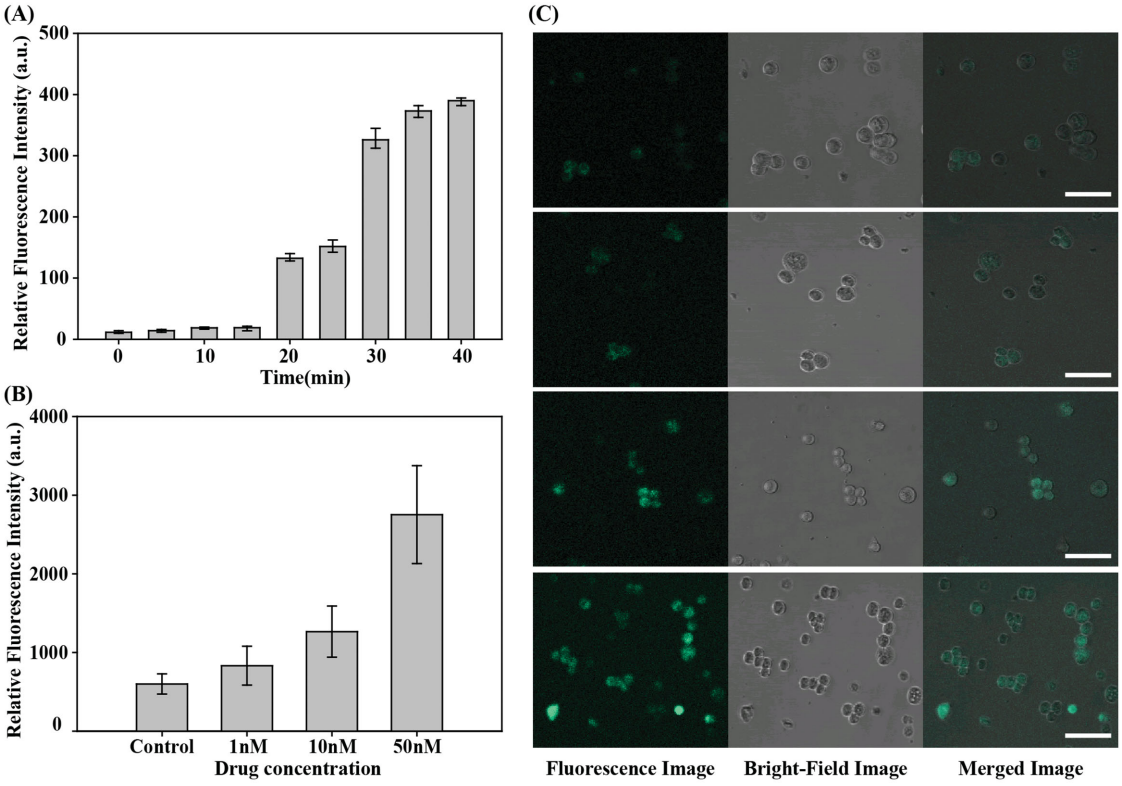

Figure 5. A) Fluorescence intensity of the cells according to the incubation time. B) Fluorescence intensities of the cells depending on the treated docetaxel concentration (0 nM, 1 nM, 10 nM, 50 nM). C) Confocal microscopy images of the docetaxel-treated cells. From top to bottom: 0 nM, 1 nM, 10 nM, 50 nM. Scale bar: 50 μm.

penetration into the nanowires could be tuned by changing the applied pressure in the manifold, and the MB-delivered cells could be detached from the nanowires and recovered by supplying a vacuum to the manifold. As opposed to previous reports, which utilized trypsin-EDTA for cellular detachment, we used a pneumatic pumping system that can physically separate the cells from the nanowire array with minimal cellular damage. Thus, the recovered cells showed a relatively high cellular viability and could be further cultured. We further demonstrated that the delivered MB in the human breast cancer MCF-7 cells could quantitatively analyze the target survivin mRNA. We expect that the proposed nanowire-incorporated microdevice can expand into the biological application arena, such as for diverse gene and drug delivery and cellular transformation by genetic engineering.

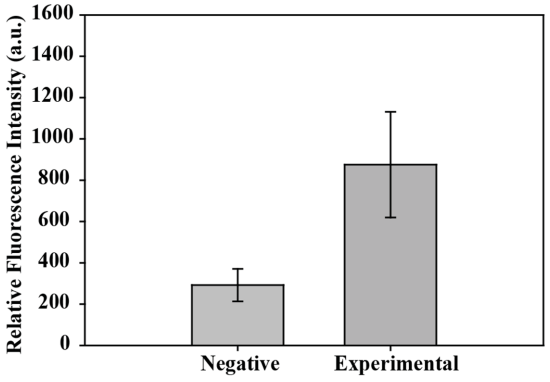

Figure 6. Plot of the cellular fluorescence intensity. The left column shows the pressure-induced MB delivery (negative control), and the right column shows the nanowire-mediated MB delivery.

4. Experimental Section

Materials: Amorphous silicon (a-Si) deposited glass wafers were purchased from Seyang Electronics (Korea). A PDMS membrane with a thickness of 250 μm was obtained from Rogers Corporation (USA). The positive photoresist (S1818) was purchased from Dow (USA). 49% Hydrofluoric acid was obtained from Avantor Performance Materials (USA). Acetone was purchased from Samchun Chemicals (Korea). Potassium hydroxide (KOH) was obtained from JUNSEI (Japan). Deionized (DI) water, DMEM, tissue culture-grade Dulbecco's phosphate-buffered saline (DPBS), fetal bovine serum (FBS), penicillin streptomycin, and trypsin-EDTA were obtained from Gibco or Invitrogen (USA). The survivin mRNA target molecular beacon and complementary DNA were synthesized from Bioneer (Korea). Human breast cancer MCF-7 cells were purchased from the Korean Cell Line Bank (Korea). PDPA was purchased from Toronto Research Chemicals (Canada). 1,1′-dioctadecyl-3,3,3′,3′-tetramethylindocarbocyanine perchlorate) (DiI), dithiothreitol (DTT), docetaxel, zinc nitrate hexahydrate ($Zn(NO_3)_2{\cdot}6H_2O$, 98%), hexamethylenetetramine (HMTA, $C_6H_{12}N_4$, 99+%), polyethyleneimine (PEI, $(C_2H_5N)_n$, low molecular weight) were purchased from Sigma-Aldrich (USA). A PD-10 separation column was purchased from GE Healthcare (USA) and an 8-well culture plate was obtained from ibidi (Germany). A Live/

DOI: 10.1002/smll.201502151

Dead cell viability assay kit was purchased from Molecular Probe of Invitrogen (USA).

Fabrication of the Microdevice: The proposed microdevice consisted of a glass manifold, a PDMS membrane (250 μm thickness), a glass channel wafer. For fabrication of a glass channel wafer and a glass manifold, a 200-nm amorphous silicon (a-Si) deposited glass wafer (1.1 mm thickness) was prepared. The design of the microchannel and manifold was patterned using a positive photoresist on a-Si deposited glass wafer using a conventional photolithography process, and a reactive ion etching (RIE) (VSRIE-400A, Vacuum Science, Korea) using SF_6 plasma was followed. The exposed glass area was wet-etched with 49% hydrofluoric acid at a depth of 100 μm (manifold) and 35 μm (microchannel). The residual photoresist was washed away with acetone and the amorphous silicon was removed with a 6 m potassium hydroxide solution. A computer numerical control (CNC) mill (SHERLINE, USA) was used to drill the holes in the manifold. To enable the injection and withdrawal of the cell solution, the PDMS membrane was punched at the same position of the inlet and outlet hole of the manifold. Before assembling the manifold, the PDMS membrane, the manifold, and the channel layer were treated with an O_2 plasma (PDC-32G, Harrick, USA) for 1 min, and then the three layers were aligned and bonded together.

Fabrication of ZnO Nanowires: ZnO nanowires were fabricated in the microchannel by a hydrothermal synthetic method.[15] A ZnO nanowire precursor solution was synthesized by mixing zinc nitrate hexahydrate, hexamethylenetetramine (HMTA) and PEI in deionized water. To form the thin ZnO seed layer on the channel, we used an RF sputtering method (150W, 3 min) with the surface masked except for the channel part. The sputtering method produced a seed layer of about 10 nm on the channel, and then the seed substrate was immersed in the precursor solution. The immersed substrate was heated at 95 °C for 2.5 h. The average diameter of the nanowires was about 36.8 nm and the average height was about 529.5 nm. The density of the ZnO nanowires could be controlled by tuning the sputtering time of the seed materials as shown in Figure S3 in the Supporting Information.

Operation of the Microdevice: The inlet and outlet holes of the manifold were connected with a syringe pump and the pump hole was linked with a pneumatic pump. Then, the assembled microdevice was positioned on the confocal microscope (Nikon, D-Eclipse, C1si). After the cells were injected into the microdevice from the inlet hole, a pneumatic pressure was applied through the manifold for pressure-induced penetration of the cells by the ZnO nanowires. The non-penetrated cells were washed away with DMEM. Five pressures (0 mbar, 4.4 mbar, 13 mbar, 40 mbar, 124 mbar) were investigated for penetration and 13 mbar was determined to be the optimal pressure. After penetration, an incubation time of 35 min was required to deliver the MBs into the cells. Finally, a reverse directional pneumatic pressure was applied to the manifold and the cells were detached and recovered from the nanowires. By injecting the media solution, the MB-delivered cells were collected from the outlet hole. Collected cells were cultured in a microwell plate.

Modification of the Nanowires: A PDPA solution was prepared with a concentration of 0.2 mM and the nanowire channel was treated with this PDPA solution for 2 h. The sequence of the MB was designed for targeting survivin mRNA and a thiol group was incorporated in the stem part for functionalization of the nanowires. As the thiol group was initially protected, 0.5 mM of a DTT solution was used for eliminating the protecting group from the thiol group in the MB. The DTT solution was mixed with the MB solution and incubated for 2 h. To purify the unprotected MB from the mixture, a PD-10 separation column was used. The purified unprotected MB was obtained and was incubated in the PDPA-treated nanowire channel for 2 h. To verify the successful conjugation of the MB on the nanowires, single-stranded DNA with a complementary base sequence to the loop sequence of MB was used as shown in **Table 1**.

Table 1. Sequence information of molecular beacon and complementary DNA.

Molecules	Sequences
Molecular Beacon	5′ – FAM-CTGAGAAAGGGCTGCCAGTCT*CAG-BHQ1 – 3′
Complementary ssDNA	5′ – CTGAGACTGGCAGCCCTTTCTCAG – 3′

*Thymine is modified with a thiol group.

Cell Preparation: Human breast cancer MCF-7 cells were used in this study and the concentration of the cell solution was 2.5×10^5 cell mL^{-1}. The cells were cultured with DMEM containing 10% FBS and 1% penicillin streptomycin and grown in a humidified 5% CO_2 incubator at 37 °C. The cells were collected by trypsin-EDTA treatment, concentrated by centrifugation, and resuspended in DMEM to be able to adjust the cell concentration.

Morphological Change and Cell Viability Assay: To observe the morphological change of the cell membrane under pressure variation, we stained the cell membrane of MCF-7 cell with 0.5% (v/v) Dil in DMEM by incubating for 10 min. To evaluate the viability of the cells, a Live/Dead cell viability assay kit, which contains acetomethoxy calcein (calcein AM) and ethidium homodimer-1, was used. After collecting the cells from the microdevice, the cells were treated by calcein AM and ethidium homodimer-1 solution with 1% concentration (v/v) for 30 min, and then the fluorescence images were taken by a confocal microscope to measure the cellular viability.

Docetaxel Treatment: Docetaxel was used as a drug to increase the survivin mRNA expression. The MCF-7 cells were treated with 0, 1, 10, and 50 nM of docetaxel for 10 h, and the fluorescence image and intensities after MB delivery were observed with a confocal microscope.

Supporting Information

Supporting Information is available from the Wiley Online Library or from the author.

Acknowledgements

This work was supported by the Engineering Research Center of Excellence Program of Korea Ministry of Science, ICT & Future Planning (MSIP)/National Research Foundation of Korea (NRF) (2014R1A5A1009799). K.H.K. and J.K. contributed equally to this work.

DOI: 10.1002/smll.201502151

[1] D. L. Sokol, X. L. Zhang, P. Z. Lu, A. M. Gewitz, *Proc. Natl. Acad. Sci. USA* **1998**, *95*, 11538.
[2] T. J. Drake, C. D. Medley, A. Sen, R. J. Rogers, W. H. Tan, *ChemBioChem* **2005**, *6*, 2041.
[3] D. P. Bratu, B. J. Cha, M. M. Mhlanga, F. R. Kramer, S. Tyagi, *Proc. Natl. Acad. Sci. USA* **2003**, *100*, 13308.
[4] S. Tyagi, O. Alsmadi, *Biophys. J.* **2004**, *87*, 4153.
[5] A. K. Chen, M. A. Behlke, A. Tsourkas, *Nucleic Acids Res.* **2009**, *37*, 11.
[6] J. A. Kim, K. C. Cho, M. S. Shin, W. G. Lee, N. C Jung, C. I. Chung, J. K. Chang, *Biosens. Bioelectron.* **2008**, *23*, 1353.
[7] M.-J. Kim, T. Kim, Y.-H. Cho, *Appl. Phys. Lett.* **2012**, *101*, 223705.
[8] M. Olbrich, E. Rebollar, J. Heitz, I. Frischauf, C. Romanin, *Appl. Phys. Lett.* **2008**, *92*, 013901.
[9] B. Qu, Y. J. Eu, W. J. Jeong, D. P. Kim, *Lab Chip* **2012**, *12*, 4483.
[10] D. S. Seferos, A. E. Prigodich, D. A. Giljohann, P. C. Patel, C. A. Mirkin, *Nano Lett.* **2009**, *9*, 308.
[11] D. S. Seferos, D. A. Giljohann, H. D. Hill, A. E. Prigodich, C. A. Mirkin, *J. Am. Chem. Soc.* **2007**, *129*, 15477.
[12] H. Y. Yeh, M. V. Yates, A. Mulchandania, W. Chen, *Chem. Commun.* **2010**, *46*, 3914.
[13] X. J. Lin, T. Konno, K. Ishihara, *Biomacromolecules* **2014**, *15*, 150.
[14] L. E. Greene, M. Law, D. H. Tan, M. Montano, J. Goldberger, G. Somorjai, P. D. Yang, *Nano Lett.* **2005**, *5*, 1231.
[15] L. E. Greene, B. D. Yuhas, M. Law, D. Zitoun, P. D. Yang, *Inorg. Chem.* **2006**, *45*, 7535.
[16] A. M. Xu, A. Aalipour, S. Leal-Ortiz, A. H. Mekhdjian, X. Xie, A. R. Dunn, C. C. Garner, N. A. Melosh, *Nat. Commun.* **2014**, *5*, 3613.
[17] F. Mumm, K. M. Beckwith, S. Bonde, K. L. Martinez, P. Sikorski, *Small* **2013**, *9*, 263.
[18] G. Ambrosini, C. Adida, D. C. Altieri, *Nat. Med.* **1997**, *3*, 917.
[19] A. Sugunan, H. C. Warad, M. Boman, J. Dutta, *J. Sol-Gel Sci. Technol.* **2006**, *39*, 49.
[20] M. Guo, P. Diao, S. Cai, *J. Solid State Chem.* **2005**, *178*, 1864.
[21] X. Chen, A. Kis, A. Zettl, C. R. Bertozzi, *Proc. Natl. Acad. Sci. USA* **2007**, *104*, 8218.
[22] E. Taratula, E. Galoppini, R. Mendelsohn, *Langmuir* **2009**, *25*, 2107.
[23] F. Q. Schafer, G. R. Buettner, *Free Radicals Biol. Med.* **2001**, *30*, 1191.
[24] K. C. Weng, C. O. Noble, B. Papahadjopoulos-Sternberg, F. F. Chen, D. C. Drummond, D. B. Kirpotin, D. H. Wang, Y. K. Hom, B. Hann, J. W. Park, *Nano Lett.* **2008**, *8*, 2851.
[25] X. H. Peng, Z. H. Cao, J. T. Xia, G. W. Carlson, M. M. Lewis, W. C. Wood, L. Yang, *Cancer Res.* **2005**, *65*, 1909.
[26] Y. Piao, F. Liu, T. S. Seo, *ACS Appl. Mater. Interfaces* **2012**, *4*, 6785.
[27] J. M. Perrier-Cornet, M. Hayert, P. Gervais, *J. Appl. Microbiol.* **1999**, *87*, 1.

Received: July 20, 2015
Revised: September 1, 2015
Published online:

DOI: 10.1002/smll.201502151